PERGAMON

Chaos, Solitons and Fractals 12 (2001) 2323–2341

CHAOS
SOLITONS & FRACTALS

www.elsevier.nl/locate/chaos

Dynamics of a Hénon–Lozi-type map

M.A. Aziz-Alaoui [a,*], Carl Robert [b], Celso Grebogi [c]

[a] *Département de mathématiques, L. M., Fac. Sc. Tech., BP 540, 76058 Le Havre Cedex, France*
[b] *Department of Physics, University of California, Santa Barbara, CA 93106, USA*
[c] *Institute for Plasma Research, Department of Mathematics and Institute for Physical Science and Technology, University of Maryland, College Park, MA 20742, USA*

Accepted 4 August 2000

Abstract

We present and analyze a smooth version of the piecewise linear Lozi map. The principal motivation for this work is to develop a map, which is better amenable for an analytical treatment as compared to the Hénon map and is one that still possesses the characteristics of a Hénon-type dynamics. This paper is a first step. It does the comparison of the Lozi map (which is a piecewise linear version of the Hénon map) with the map that we introduce. This comparison is done for fixed parameters and also through global bifurcation by changing a parameter. If ε measures the degree of smoothness, we prove that, as $\varepsilon \to 0$, the stability and the existence of the fixed points are the same for both maps. We also numerically compare the chaotic dynamics, both in the form of an attractor and of a chaotic saddle.

1. Introduction

Even the simplest nonlinear maps on $\mathbb{R}^2$, like Hénon's map [8],

$$\mathscr{H}_{a,b}:\begin{pmatrix}x\\y\end{pmatrix}\to\begin{pmatrix}1-ax^2+y\\bx\end{pmatrix},$$

$a,b\in\mathbb{R},\ b\neq 0$, are extremely difficult to analyze. One way to avoid technical problems and to overcome difficulties is to study piecewise linear maps which are in close approximation to the nonlinear maps one wants to investigate. Often, mathematical analysis tends to be easier for piecewise linear maps than smooth nonlinear ones. This is possible because linearity on parts of the domain enables for effective calculations. The work of Lozi [10] on the Hénon map follows this idea and gave rise to the well-known Lozi map. It is a two-parameter family of piecewise affine homeomorphism of the plane into itself,

$$\mathscr{L}_{a,b}:\begin{pmatrix}x\\y\end{pmatrix}\to\begin{pmatrix}1-a|x|+y\\bx\end{pmatrix},$$

$a,b\in\mathbb{R},\ b\neq 0$. This modification of Hénon's map makes the transformation linear on both domains $x>0$ and $x<0$. This allowed Misiurewicz [11] to prove the conjecture of Lozi about the existence of a chaotic

* Corresponding author.
E-mail address: aziz@univ-lehavre.fr (M.A. Aziz-Alaoui).

0960-0779/01/$ - see front matter
PII: S0960-0779(00)00192-2

attractor for the Lozi map and its hyperbolicity. This feature leads to sensitive dependence on initial conditions, which is a characterization of chaos. However, by making such an approximation, there is a loss of smoothness, which prevents application of known results from dynamics, like the standard bifurcation theory. Indeed Lozi's map is not everywhere differentiable. Its hyperbolic structure can be understood only as the existence of a hyperbolic splitting at those points at which it may exist. This splitting cannot be extended to a continuous one on the whole plane (see, for example, a smooth version of some maps which is studied in [1]).

In the present work, we approximate the Lozi map

$$\mathscr{L}_{a,b} = \mathscr{L}_{a,b,0}$$

by a C^1 smooth map $\mathscr{L}_{a,b,\varepsilon}$ (see [2]), and study which properties are preserved after the smoothing procedure. We find that this map shares many of the qualitative features of both Lozi's and Hénon's maps. Consider the map:

$$\mathscr{L}_{a,b,\varepsilon} : \begin{pmatrix} x \\ y \end{pmatrix} \to \begin{pmatrix} 1 - aS_\varepsilon(x) + y \\ bx \end{pmatrix}, \tag{1}$$

where $a, b \in \mathbb{R}$, $b \neq 0$ and $S_\varepsilon(x)$ is defined by

$$S_\varepsilon : \mathbb{R} \to \mathbb{R}, \quad x \to S_\varepsilon(x) = \begin{cases} |x| & \text{if } |x| \geqslant \varepsilon, \\ g_\varepsilon(x) = (x^2/2\varepsilon) + (\varepsilon/2) & \text{if } |x| \leqslant \varepsilon, \end{cases} \tag{2}$$

where ε satisfies

$$0 < \varepsilon < 1. \tag{3}$$

The only difference between Hénon's (or Lozi's) transformation is that the term x^2 (or $|x|$) is replaced by $S_\varepsilon(x)$. But we clearly have

$$\lim_{\varepsilon \to 0^+} S_\varepsilon(x) = |x|.$$

Fig. 1 shows the graph of $S_\varepsilon(x)$ for $\varepsilon = 0.01$ and $\varepsilon = 0.5$.

The main objective of this paper is to provide a basic analysis of $\mathscr{L}_{a,b,\varepsilon}$ along with detailed comparison with the Lozi map when $\varepsilon \to 0$. It is not our goal here to compare $\mathscr{L}_{a,b,\varepsilon}$ with the Hénon map. This will be the object of the following paper.

We first present general properties of $\mathscr{L}_{a,b,\varepsilon}$. We then analyze its local and global dynamics. Finally, we discuss some numerical investigations. Throughout the text, a constant comparison with Lozi's map is being done.

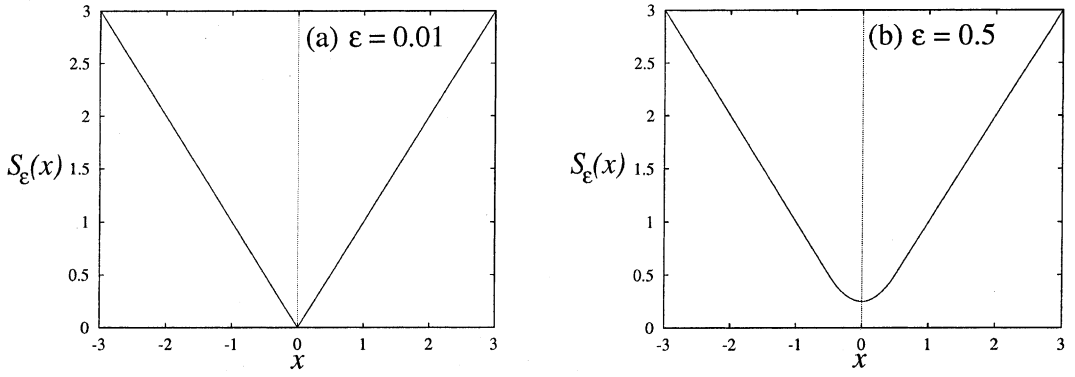

Fig. 1. Graph of the function S_ε for: (a) $\varepsilon = 0.01$; (b) $\varepsilon = 0.5$.

2. Some properties of $\mathscr{L}_{a,b,\varepsilon}$

2.1. Generalities

The function $S_\varepsilon(x)$ is continuous. It is, in fact, $C^1(\mathbb{R})$, its first derivative with respect to x is

$$\frac{\partial S_\varepsilon(x)}{\partial x} = \begin{cases} 1 & \text{if } x \geqslant \varepsilon, \\ x/\varepsilon & \text{if } |x| \leqslant \varepsilon, \\ -1 & \text{if } x \leqslant -\varepsilon \end{cases} \tag{4}$$

and

$$\lim_{x \to \varepsilon^{\pm}} \frac{\partial S_\varepsilon}{\partial x}(x) = 1 \quad \text{and} \quad \lim_{x \to -\varepsilon^{\pm}} \frac{\partial S_\varepsilon}{\partial x}(x) = -1.$$

The map $\mathscr{L}_{a,b,\varepsilon}$ is a diffeomorphism when $b \neq 0$. Indeed its Jacobian matrix at point X is given by

$$D_{\mathscr{L}_{a,b,\varepsilon}}(X) = \begin{pmatrix} -a\frac{\partial S_\varepsilon(x)}{\partial x} & 1 \\ b & 0 \end{pmatrix}, \tag{5}$$

and its determinant is nonzero if $b \neq 0$. Therefore the mapping $\mathscr{L}_{a,b,\varepsilon}$ is area-preserving when $b = -1$. It preserves area but reverses orientation when $b = 1$, as the Hénon map does. Moreover if $a = 0$, this mapping reduces to a linear map. Thus, we assume throughout this paper that $a \neq 0$ and $b \neq 0$.

Since our aim is a comparison between the Lozi map and $\mathscr{L}_{a,b,\varepsilon}$, we start by recalling some results on the Lozi mapping. For this map, simple algebraic computations show that the fixed points occur at

$$\Pi_1 = \left(\bar{x}_1, \bar{y}_1\right) = \left(\frac{1}{1+a-b}, \frac{b}{1+a-b}\right)$$

if $b < a + 1$; and

$$\Pi_2 = \left(\bar{x}_2, \bar{y}_2\right) = \left(\frac{1}{1-a-b}, \frac{b}{1-a-b}\right)$$

if $b > 1 - a$ (see Fig. 2(a)). Furthermore, one can easily determine the local stability of these points by evaluating the eigenvalues of the Jacobian matrix of the Lozi map

$$D_{\mathscr{L}_{a,b,0}}(X) = \begin{pmatrix} -a\frac{\partial |x|}{\partial x} & 1 \\ b & 0 \end{pmatrix},$$

at these fixed points. The characteristic equation computed from this Jacobian is

$$\lambda^2 + a\lambda - b = 0 \quad \text{for } \Pi_1, \qquad \lambda^2 - a\lambda - b = 0 \quad \text{for } \Pi_2. \tag{6}$$

The stability of Π_1 and Π_2 is then summarized in Fig. 3(a). If both the eigenvalues obey $|\lambda^{\pm}| < 1$, then the fixed points are asymptotically stable and are sinks. Here it is the case of Π_1, this occurs in the triangle $b > -1$, $b < a + 1$ and $b < -a + 1$. If both the eigenvalues obey $|\lambda^{\pm}| > 1$, then the fixed points are unstable, and are therefore sources. Here it occurs for Π_1 if $b < -1$, $b < a + 1$ and $b < -a + 1$ and for Π_2 in its entire domain of existence. When one of the eigenvalues is such that $|\lambda_1| < 1$ and the other such that $|\lambda_2| > 1$, the fixed point is a saddle. This occurs for Π_1 and Π_2 in the domain where they coexist, that is if $b < a + 1$ and $b > -a + 1$. For more details on the Lozi family, see for example [9,16–18]. See also [3,19–21] and references therein for recent results on Hénon's map.

We shall use various notations and assumptions on the parameters a and b. We list them below (see also Fig. 2).

(i) $\mathscr{B}_1$ is the bend of (a,b)-plane defined by $\mathscr{B}_1 = \{(a,b) \in \mathbb{R}^2,\ b < a + 1 \leqslant b + 1/\varepsilon\}$.
(ii) $\mathscr{B}_2$ is the bend of (a,b)-plane defined by $\mathscr{B}_2 = \{(a,b) \in \mathbb{R}^2,\ b - 1/\varepsilon \leqslant -a + 1 < b\}$.
(iii) The quadrant $\mathscr{Q}_0 = \{(a,b) \in \mathbb{R}^2,\ a + 1 < b < -a + 1\}$.

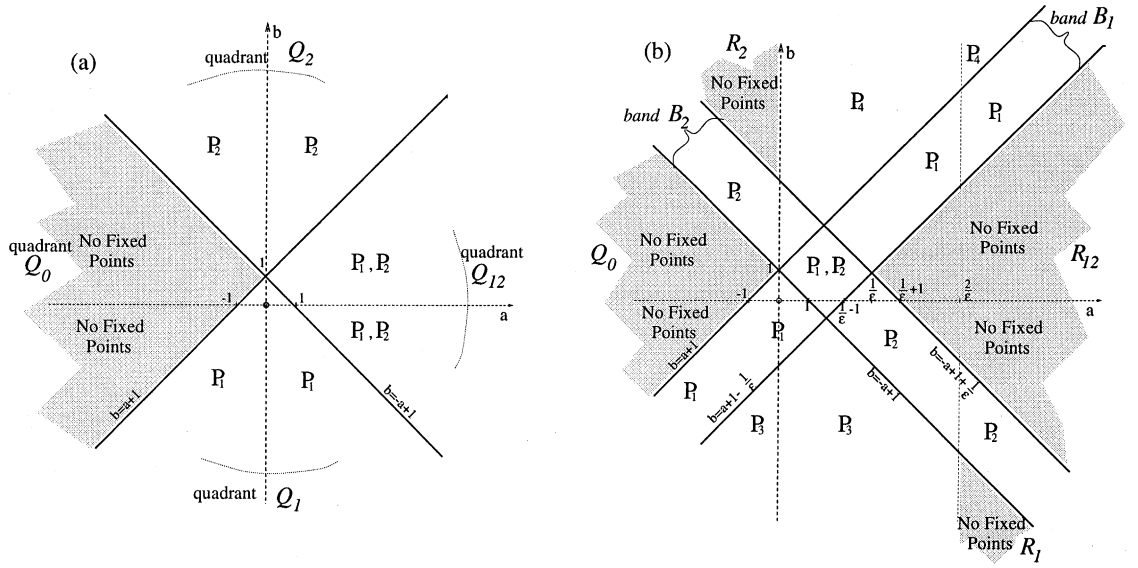

Fig. 2. Comparison of the Lozi and $\mathscr{L}_{a,b,\varepsilon}$ mappings: (a) fixed points of the Lozi mapping; (b) fixed points of the $\mathscr{L}_{a,b,\varepsilon}$ mapping.

(iv) The quadrant $\mathscr{Q}_1 = \{(a,b) \in \mathbb{R}^2,\ b < a+1 \text{ and } b < -a+1\}$.
(v) The quadrant $\mathscr{Q}_{12} = \{(a,b) \in \mathbb{R}^2,\ -a+1 < b < a+1\}$.
(vi) The quadrant $\mathscr{Q}_2 = \{(a,b) \in \mathbb{R}^2,\ b > -a+1 \text{ and } b > a+1\}$.
(vii) The region $\mathscr{R}_1 = \{(a,b) \in \mathbb{R}^2,\ b < -a+1 \text{ and } a > 2/\varepsilon\}$.
(viii) The region $\mathscr{R}_{12} = \{(a,b) \in \mathbb{R}^2, -a+1+1/\varepsilon < b < a+1-1/\varepsilon\}$.
(ix) The region $\mathscr{R}_2 = \{(a,b) \in \mathbb{R}^2,\ b > -a+1+1/\varepsilon \text{ and } b < 0\}$.

2.2. Local behavior

In this section, we give the fixed points of $\mathscr{L}_{a,b,\varepsilon}$, their stability type with respect to the stability type of the fixed points of the Lozi map, and the geometry of the stable and unstable manifolds of the saddle points. Our aim is to prove that, for ε small enough, in the large region of the (a,b)-plane, these two maps have the same simple behavior. We begin by studying the existence of the fixed points of $\mathscr{L}_{a,b,\varepsilon}$ mapping.

Proposition 1.
(1) (i1) *If* $(a,b) \in \mathscr{B}_1$, *then there is a fixed point at*

$$P_1 = (\bar{x}_1, \bar{y}_1) = \left(\frac{1}{1+a-b}, \frac{b}{1+a-b} \right).$$

(i2) *If* $(a,b) \in \mathscr{B}_2$, *then there is a fixed point at*

$$P_2 = (\bar{x}_2, \bar{y}_2) = \left(\frac{1}{1-a-b}, \frac{b}{1-a-b} \right).$$

(2) *If* $a \in \mathbb{R} \setminus]0, 2/\varepsilon[$, *define* $\alpha^{\pm}(a) = 1 \pm \sqrt{a^2 - (2a/\varepsilon)}$. *Assume* $(a \in [0, 2/\varepsilon])$ *or* $(a \in]-\infty, 0[\cup]2/\varepsilon, +\infty[$ *and* $(b \leqslant \alpha^-(a)$ *or* $b \geqslant \alpha^+(a)))$, *then*:
(j1) *If* $(a,b) \in \mathscr{Q}_1 \setminus \mathscr{B}_1$ *and* $a \leqslant (2/\varepsilon)$, *there is a fixed point at* $P_{3,\varepsilon} = (\bar{x}_3, \bar{y}_3)$, *where*

$$\bar{x}_3 = \frac{\varepsilon}{a}\left(b - 1 - \sqrt{(1-b)^2 - a^2 + \frac{2a}{\varepsilon}} \right), \quad \bar{y}_3 = b\bar{x}_3.$$

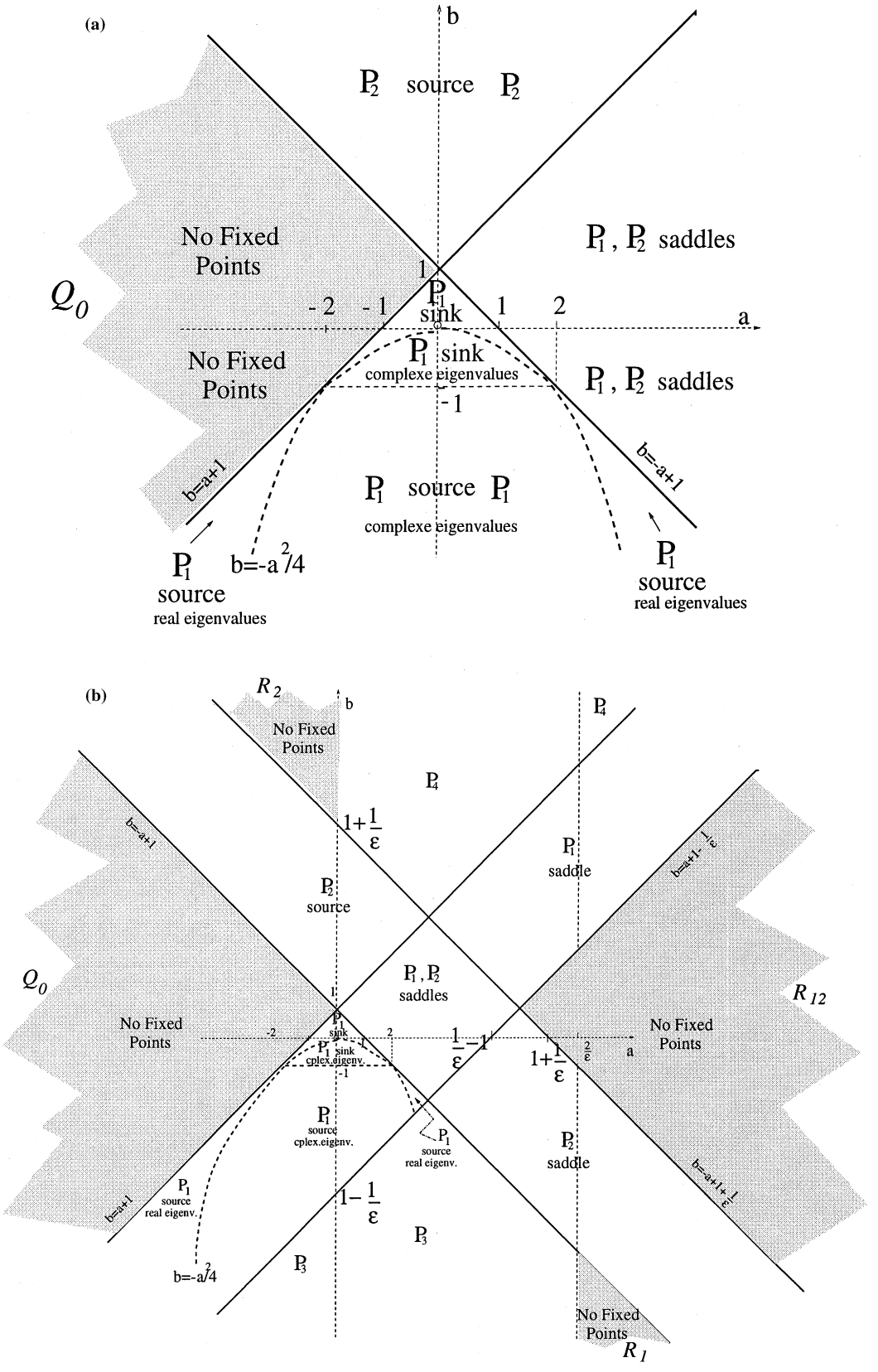

Fig. 3. (a) Stability of the fixed points of the Lozi map. (b) Stability of the fixed points of $\mathscr{L}_{a,b,\varepsilon}$.

(j2) *If* $(a,b) \in \mathscr{Q}_2 \setminus \mathscr{B}_2$ *and* $a > 0$, *there is a fixed point at* $P_{4,\varepsilon} = (\bar{x}_4, \bar{y}_4)$ *where*

$$\bar{x}_4 = \frac{\varepsilon}{a}\left(b - 1 + \sqrt{(1-b)^2 - a^2 + \frac{2a}{\varepsilon}}\right), \quad \bar{y}_4 = b\bar{x}_4.$$

(j3) *The region* $\mathscr{R}_0 = \mathscr{Q}_0 \cup \mathscr{R}_1 \cup \mathscr{R}_{12} \cup \mathscr{R}_2$ *contains no fixed points.*

Proof. The fixed points of $\mathscr{L}_{a,b,\varepsilon}$ are the real solutions of the system:

$$1 - aS_\varepsilon(x) + y = x, \quad bx = y. \tag{7}$$

Hence, one may easily obtain the equation

$$aS_\varepsilon(x) + x(1-b) - 1 = 0, \tag{8}$$

which is equivalent to the system:

$$a|x| + x(1-b) - 1 = 0 \quad \text{if } |x| \geqslant \varepsilon, \qquad \frac{a}{2\varepsilon}x^2 + (1-b)x + \frac{a\varepsilon}{2} - 1 = 0 \quad \text{if } |x| \leqslant \varepsilon. \tag{9}$$

(1) If $x \geqslant \varepsilon$, then, from the system above, we get $ax + x(1-b) - 1 = 0$, then $x = x_1 = 1/(1+a-b)$ is the solution if the condition $x = x_1 \geqslant \varepsilon$ is satisfied, that is if the condition $(a,b) \in \mathscr{B}_1$ given in Proposition 1(i1) is satisfied.

If $x \leqslant -\varepsilon$, then from the system above, we get the equation $ax - x(1-b) + 1 = 0$, and $x = x_2 = 1/(1-a-b)$ is the abscissa of the second fixed point if the condition $x = x_2 \leqslant -\varepsilon$ holds, that is if the condition $(a,b) \in \mathscr{B}_2$ given in Proposition 1(i2) is satisfied. That determines the two fixed points P_1 and P_2 (see Fig. 2). Notice that these fixed points are the same as those of the Lozi map ($P_1 = \Pi_1$ and $P_2 = \Pi_2$).

(2) (j1)–(j2) If $|x| \leqslant \varepsilon$, solutions of Eq. (7) are obtained by solving the equation

$$T_\varepsilon(x) = \frac{a}{2\varepsilon}x^2 + x(1-b) + \frac{a\varepsilon}{2} - 1 = 0. \tag{10}$$

This equation has real solutions if $\Delta = (b-1)^2 - a^2 + (2a/\varepsilon) \geqslant 0$. This condition holds if and only if one of the following conditions is also satisfied:

$$a \in \left[0, \frac{2}{\varepsilon}\right] \quad \text{or} \quad \left(a \in \mathbb{R} \setminus \left[0, \frac{2}{\varepsilon}\right]\right) \text{ and } (b \leqslant \alpha^-(a) \text{ or } b \geqslant \alpha^+(a)), \tag{11}$$

where $\alpha^\pm(a) = 1 \pm \sqrt{a^2 - (2a/\varepsilon)}$.

Solutions of Eq. (10) are

$$x^\pm = \frac{\varepsilon}{a}\left(b - 1 \mp \sqrt{(b-1)^2 - a^2 + \frac{2a}{\varepsilon}}\right). \tag{12}$$

But these abscissa must verify $|x^\pm| \leqslant \varepsilon$, that is

$$\left|b - 1 \mp \sqrt{(b-1)^2 - a^2 + \frac{2a}{\varepsilon}}\right| \leqslant |a|. \tag{13}$$

Finally, from (11) and (13), simple algebraic calculations show that conditions (2)(j1) and (2)(j2) given in Proposition 1 are necessary for the existence of solutions of (10) with $|x| \leqslant \varepsilon$.

(Let us remark that if $a > 2/\varepsilon$, $P_{3,\varepsilon}$ cannot exist, since if $\Delta = (b-1)^2 - a^2 + (2a/\varepsilon) \geqslant 0$ and $a > 0$, the condition $|\bar{x}_3| \leqslant \varepsilon$ implies that $b > a + 1$ and $b \leqslant a + 1 - 1/\varepsilon$; on the other hand, as $\Delta \geqslant 0$, we get $\alpha^+(a) \leqslant b$; thus, as $\alpha^+(a) < a + 1 - (1/\varepsilon)$, the condition $b \leqslant a + 1 - 1/\varepsilon$, necessary to have $|\bar{x}_3| \leqslant \varepsilon$ could not be satisfied. Similar remark holds for $P_{4,\varepsilon}$, if $a < 0$, since $\alpha^-(a) > a + 1 - (1/\varepsilon)$).

Consequently, the two last possible fixed points of $\mathscr{L}_{a,b,\varepsilon}$ have the abscissas $\bar{x}_3 = x^-$ and $\bar{x}_4 = x^+$.

(2)(j3) The last result of this proposition is a corollary of the both previous ones, since these propositions set that there is no other fixed points but P_1, P_2 and $P_{3,\varepsilon}$, $P_{4,\varepsilon}$, and they do not exist when (a,b) is in region $\mathscr{R}_0$. □

Fig. 3 gives the fixed points and their type in the Lozi and $\mathscr{L}_{a,b,\varepsilon}$ mappings and their location, for all reals a and b and for $0 < \varepsilon < 1$. One can notice that when ε approaches 0, the lines $b = a + 1 - (1/\varepsilon)$ and $b = -a + 1 + (1/\varepsilon)$ are translated far away to the right (to infinity), thus Fig. 2(b) becomes similar to Fig. 2(a). That is, the fixed points $P_{3,\varepsilon}$ and $P_{4,\varepsilon}$ of the $\mathscr{L}_{a,b,\varepsilon}$ mapping disappear when $\varepsilon \to 0$, so the number of fixed points in the Lozi and $\mathscr{L}_{a,b,\varepsilon}$ mappings becomes the same.

Proposition 2. *Assume that* $(a,b) \in \mathscr{B}_1$ (*so* P_1 *exists*).

1. P_1 *is a sink if and only if* $b > -1$ *and* $(a,b) \in \mathscr{Q}_1$. *It has real eigenvalues if* $b \geqslant -a^2/4$, *and complex eigenvalues for* $b < -a^2/4$.
2. P_1 *is a source if and only if* $b < -1$ *and* $(a,b) \in \mathscr{Q}_1$. *It has real eigenvalues if* $b \geqslant -a^2/4$, *and complex eigenvalues for* $b < -a^2/4$.
3. P_1 *is a saddle if and only if* $(a,b) \in \mathscr{Q}_{12}$.

Fig. 3(b) illustrates this proposition.

Proof. The eigenvalues of $D_{\mathscr{L}_{a,b,\varepsilon}}(P_1)$ (the derivative of $\mathscr{L}_{a,b,\varepsilon}$ at P_1, given by (5)) are solutions of the characteristic equation

$$\lambda^2 + a\lambda \frac{\partial S_\varepsilon(\bar{x}_1)}{\partial x} - b = 0, \tag{14}$$

where $\frac{\partial S_\varepsilon(\bar{x}_1)}{\partial x}$ is given by (4), thus, as $x \geqslant \varepsilon$ for P_1, we get

$$\lambda^2 + a\lambda - b = 0. \tag{15}$$

The eigenvalues are then

$$\lambda_1^{\pm} = \frac{1}{2}\left[-a \pm \sqrt{a^2 + 4b} \right]. \tag{16}$$

Consequently, after some algebraic computations one obtains the following results:

• If $a^2 + 4b \geqslant 0$, then the eigenvalues are real and

(i) $|\lambda_1^+| < 1$ if and only if

$$(a \in]-2,2[\text{ and } b < a+1) \quad \text{or} \quad (a \geqslant 2 \text{ and } -a+1 < b < a+1),$$

(ii) $|\lambda_1^-| < 1$ if and only if

$$(a \in]-2,2[\text{ and } b < -a+1) \quad \text{or} \quad (a \leqslant -2 \text{ and } a+1 < b < -a+1),$$

(iii) $|\lambda_1^+| > 1$ if and only if

$$(a < -2) \quad \text{or} \quad (a > 2 \text{ and } b < -a+1),$$

(iv) $|\lambda_1^-| > 1$ if and only if

$$(a < -2 \text{ and } b < a+1) \quad \text{or} \quad (a > 2) \quad \text{or} \quad (a \leqslant 2 \text{ and } b > -a+1).$$

• If $a^2 + 4b < 0$, then the eigenvalues are complexes. In this case, $|\lambda_1^{\pm}| < 1$ if and only if $-1 < b < -a^2/4$ and $|\lambda_1^{\pm}| > 1$ if and only if $b < -1$ and $b < -a^2/4$.

Consequently:

(1) *For* P_1 *to be a sink* (i.e., $|\lambda_1^{\pm}| < 1$):

If $a^2 + 4b \geqslant 0$, then the eigenvalues are real and conditions (i) and (ii) must be verified. If, moreover, we take into account conditions of existence of P_1, this leads to conditions $(a \in]-2,2[$, $b < a+1$ and $b < -a+1)$.

If $a^2 + 4b < 0$, then the eigenvalues are complex, then $|\lambda_1^{\pm}| < 1$, if and only if $-1 < b < -a^2/4$.

Consequently, P_1 is a sink if $(a,b) \in \mathscr{B}_1 \cap \mathscr{Q}_1$ and $b > -1$.

(2) P_1 *is a source if* $|\lambda_1^{\pm}| > 1$:

If $a^2 + 4b \geqslant 0$, then the eigenvalues are real, conditions (iii) and (iv) must be verified, which can be simplified to obtain ($a < 2$ and $b < a + 1$) or ($a > 2$ and $b < -a + 1$) if we take into account conditions for the existence of P_1.

If $a^2 + 4b < 0$, then the eigenvalues are complex, $|\lambda_1^{\pm}| > 1$, if and only if $b < -1$ and $b < -a^2/4$.

Consequently, P_1 is a source if $(a, b) \in \mathscr{B}_1 \cap \mathscr{Q}_1$ and $b < -1$.

(3) A saddle fixed point occurs when one eigenvalue is less than one and the other greater than one in modulus. Assume that $a^2 + 4b \geqslant 0$. P_1 is a saddle if conditions (i, iv) or (ii, iii) are verified, then if the following conditions hold, ($a \in]-2, 2[$, $b < a + 1$ and $b > -a + 1$) or ($a > 2$ and $-a + 1 < b < a + 1$). If moreover we take into account conditions of existence of P_1, this implies that $(a, b) \in \mathscr{B}_1 \cap \mathscr{Q}_{12}$.

(If $a^2 + 4b < 0$, $|\lambda_1^{\pm}|$ are both >1 or both <1, then no saddle type is possible). □

Proposition 3. *Assume that* $(a, b) \in \mathscr{B}_2$ (*so* P_2 *exists*).

(1) P_2 *is always unstable.*

(2) P_2 *is a source if and only if* $(a, b) \in \mathscr{Q}_2$.

(3) P_2 *is a saddle if and only if* $(a, b) \in \mathscr{Q}_{12}$.

Proof. The characteristic equation computed from the Jacobian matrix $D_{\mathscr{L}_{a,b,\varepsilon}}(P_2)$ is also given by Eq. (14). As for P_2, $x \leqslant -\varepsilon$ and this equation becomes

$$\lambda^2 - a\lambda - b = 0. \tag{17}$$

The eigenvalues are then

$$\lambda_2^{\pm} = \frac{1}{2}\left[a \pm \sqrt{a^2 + 4b}\right]. \tag{18}$$

In the case $a^2 + 4b < 0$, P_2 does not exist since it exists in $\mathscr{B}_2$ only, and, obviously, $b = -a^2/4 \leqslant -a + 1$ ($-a + 1$ is the lower border of $\mathscr{B}_2$), see Proposition 1 and Fig. 2, thus, we assume $a^2 + 4b \geqslant 0$. Some algebraic computations lead to the following results:

(i) $|\lambda_2^+| < 1$ if and only if

$$(a \in]-2, 2[\text{ and } b < -a + 1) \quad \text{or} \quad (a \geqslant -2 \text{ and } a + 1 < b < -a + 1),$$

(ii) $|\lambda_2^-| < 1$ if and only if

$$(a \in]-2, 2[\text{ and } b < a + 1) \quad \text{or} \quad (a \leqslant 2 \text{ and } b > -a + 1),$$

(iii) $|\lambda_2^+| > 1$ if and only if

$$(a > 2) \quad \text{or} \quad (a \leqslant 2 \text{ and } b > -a + 1) \quad \text{or} \quad (a < -2 \text{ and } b < a + 1)$$

(iv) $|\lambda_2^-| > 1$ if and only if

$$(a > 2 \text{ and } b < -a + 1) \quad \text{or} \quad (a < -2) \text{ or } (a \geqslant -2 \text{ and } b > a + 1).$$

Thus:

1. From (i) one can see that $|\lambda_2^+| < 1$ is not possible in the domain of existence of P_2, we obviously have $|\lambda_2^+| > 1$ in this domain. That is, P_2 is an unstable fixed point.
2. As P_2 is a source if $|\lambda_2^{\pm}| > 1$, thus conditions (iii) and (iv) must be verified, which can be simplified to obtain, ($a > 2$ and $b > a + 1$) or ($a < -2$ and $b > -a + 1$) or ($a \in [-2, 2]$, $b > -a + 1$ and $b > a + 1$), if we take into account conditions of existence of P_2. These last conditions yield $(a, b) \in \mathscr{B}_2 \cap \mathscr{Q}_2$.
3. P_2 is a saddle if $|\lambda_2^-| < 1$ (since $|\lambda_2^+|$ is always > 1). Thus, for this to happen, condition (ii) must be verified. If we take into account conditions of existence of P_2, then we get $(a, b) \in \mathscr{B}_2 \cap \mathscr{Q}_{12}$. □

Lemma 1. *Let g be a mapping of the plane into itself,* $(x, y) \mapsto g(x, y) = (by + u(x), x)$, *where u is a continuous function on* $\mathbb{R}$. *If g has no fixed points, then it has no periodic points.*

Proof. It is equivalent to show that if g has a periodic point, it has a fixed point. Assume then that g has a p-periodic fixed point ($p \geqslant 1$), that is $g^p(x_0, y_0) = (x_0, y_0)$ for some $(x_0, y_0) \in \mathbb{R}^2$ (where $g^p = g \circ g \cdots \circ g$, p-times). $\{(x_i, y_i), i = 0, \ldots, p-1\}$ is then a p-periodic orbit for g.

It is sufficient to show that the diagonal $\Delta = \{(x,x) | x \in \mathbb{R}\}$ intersects $g(\Delta)$, since any point in the intersection is fixed for g.

One can see that,

$$\begin{aligned}
&(x_1, y_1) = g(x_0, y_0) = (by_0 + u(x_0), x_0),\\
&(x_{k+1}, y_{k+1}) = g(x_k, y_k) = (by_k + u(x_k), x_k) \quad \text{for } k = 1, \ldots, p-2,\\
&(x_p, y_p) = (x_0, y_0) = g(x_{p-1}, y_{p-1}) = (by_{p-1} + u(x_{p-1}), x_{p-1}).
\end{aligned} \tag{19}$$

Due to the definition of g $(g(x,y) = (by + u(x), x))$, we get

$$y_{k+1} = x_k \text{ for } k = 0, \ldots, p-1, \quad x_p = x_0 \quad \text{and} \quad y_p = y_0 = x_{p-1}.$$

All points (x_k, x_k) lie on Δ. Using Eq. (19) above, let us compute their image under g,

$$\begin{aligned}
g(x_0, x_0) &= (bx_0 + u(x_0), x_0) = (by_0 + u(x_0), x_0) + (bx_0 - by_0, 0)\\
&= (x_1, x_0) + (bx_0 - by_0, 0),\\
g(x_k, x_k) &= (bx_k + u(x_k), x_k) = (by_k + u(x_k), x_k) + (bx_k - by_k, 0)\\
&= (x_{k+1}, x_k) + (bx_k - bx_{k-1}, 0) \quad \text{for } k = 1, \ldots, p-2,\\
g(x_{p-1}, x_{p-1}) &= g(y_0, y_0) = (bx_{p-1} + u(x_{p-1}), x_{p-1})\\
&= (by_{p-1} + u(x_{p-1}), x_{p-1}) + (bx_{p-1} - by_{p-1}, 0)\\
&= (x_p, x_{p-1}) + (by_0 - bx_{p-2}, 0).
\end{aligned}$$

Thus,

$$\frac{1}{p}\sum_{k=0}^{p-1} g(x_k, x_k) = \left(\frac{1}{p}(x_0 + x_1 + \cdots + x_{p-1}), \frac{1}{p}(x_0 + x_1 + \cdots + x_{p-1})\right) + (0,0),$$

which is the position vector of the centroid of the points $g(x_i, x_i)$. Obviously this vector-sum lies on Δ. Thus, either all of the points $g(x_i, x_i)$ lie on Δ, or some two lie on opposite sides of Δ. Consequently $g(\Delta)$ intersects Δ, and g has a fixed point. □

Proposition 4. *In the region $\mathscr{R}_0$ of the (a,b)-plane defined by $\mathscr{R}_0 = \mathscr{Q}_0 \cup \mathscr{R}_1 \cup \mathscr{R}_{12} \cup \mathscr{R}_2$, all points escape to infinity under iterations by $\mathscr{L}_{a,b,\varepsilon}$.*

Proof. This proposition is a corollary of the previous propositions and Lemma 1. In order to apply the previous lemma, we first note that the transformation $\mathscr{L}_{a,b,\varepsilon}$ can be equivalently written: $\mathscr{L}_{a,b,\varepsilon}(x', y') = (1 - aS_\varepsilon(x') + by', x')$, where $x = x'$ and $y = by'$, thus $\mathscr{L}_{a,b,\varepsilon}(x', y') = (by' + u(x'), x')$, where $u(x') = 1 - aS_\varepsilon(x')$.

As $\mathscr{R}_0$ contains no fixed points (Proposition 1), it contains no periodic points (Lemma 1). Thus, as a consequence of the Brouwer theorem, if $(a,b) \in \mathscr{R}_0$, all points escape to infinity under iterations by $\mathscr{L}_{a,b,\varepsilon}$.

Let us remark that $\mathscr{R}_0$ reduces to $\mathscr{Q}_0$ when $\varepsilon \to 0$, since the borders of $\mathscr{R}_1$, $\mathscr{R}_{12}$ and $\mathscr{R}_2$ move to infinity, as $\varepsilon \to 0$, these regions then disappear. □

Proposition 5. *As $\varepsilon \to 0$, the number, existence and stability of the fixed points of both Lozi and $\mathscr{L}_{a,b,\varepsilon}$ mappings are the same (in 'almost' all the (a,b)-plane).*

Proof. This result is a corollary of the previous propositions. Indeed we have $P_1 = \Pi_1$ and $P_2 = \Pi_2$. But in this case, as $\varepsilon \to 0$, the lines $b = \pm a + 1 \mp (1/\varepsilon)$ are clearly translated to the infinity on the right of the (a,b)-plane, This is also true for the regions of the (a,b)-plane where $P_{3,\varepsilon}$ and $P_{4,\varepsilon}$ exist. That is, as $\varepsilon \to 0$,

the region $\{(a,b)\in\mathbb{R}^2,\ a+1-(1/\varepsilon)\leqslant b\leqslant -a+1+(1/\varepsilon)\}$ fills all the (a,b)-plane. Consequently, the regions allowing $P_{3,\varepsilon}$ and $P_{4,\varepsilon}$ disappear. Thus, $\mathscr{L}_{a,b,\varepsilon}$ ($\varepsilon\ll 0$) exhibits only two fixed points (P_1 and P_2) equal to those of Lozi map (Π_1 and Π_2), in almost all the (a,b)-plane (see Fig. 2).

Furthermore, P_1 (respectively, P_2) exists and has the same nature in the same region of parameters of the (a,b)-plane as Π_1 (respectively, Π_2), since, the half band $\mathscr{B}_1\cap\mathscr{Q}_1$ (respectively, $\mathscr{B}_2\cap\mathscr{Q}_2$), where it is a sink (respectively, a source), as $\varepsilon\to 0$, fills all the region $\mathscr{Q}_1$ (respectively, $\mathscr{Q}_2$), which is the domain allowing the existence of Π_1 (respectively, Π_2).

Similar reasoning works for the region $\mathscr{B}_1\cap\mathscr{B}_2$, where $P_{1,2}$ exist and are both saddles (see Proposition 2 and Fig. 2(b)). This region, when $\varepsilon\to 0$, fills all the region $\mathscr{Q}_{12}$ domain of existence and of the saddle nature of Π_i and P_i $(i=1,2)$.

Finally, the regions $\mathscr{R}_1$, $\mathscr{R}_{12}$ and $\mathscr{R}_2$ as well as the regions $\mathscr{B}_1\cap\{(a,b)\in\mathbb{R}^2,\ b\geqslant -a+1+(1/\varepsilon)\}$ and $\mathscr{B}_2\cap\{(a,b)\in\mathbb{R}^2,\ b\leqslant a+1-(1/\varepsilon)\}$ disappear as $\varepsilon\to 0$.

In conclusion, both Lozi and $\mathscr{L}_{a,b,\varepsilon}$ mappings have (for $\varepsilon\ll 0$) in 'almost' all the (a,b)-plane (especially in the region where the parameters a and b are classically chosen for Loziś (or Hénonś) maps) identical fixed points with the same type. Their orbits which escape to infinity, are for the same region of parameters $\mathscr{Q}_0$. □

2.3. Simple global behavior

In this section, we use the classical notation, $\mathscr{W}^{\mathrm{s}}(P_i)$ for the stable manifold of P_i and $\mathscr{W}^{\mathrm{u}}(P_i)$ for the unstable manifold.

Proposition 6. *Let $\mathscr{S}$ be the square $S_1S_2S_3S_4$ of the (a,b)-plane, with $S_1=(-1,0)^{\mathrm{T}}$, $S_2=(0,1)^{\mathrm{T}}$, $S_3=(0,-1)^{\mathrm{T}}$ and $S_4=(1,0)^{\mathrm{T}}$. If $(a,b)\in\mathscr{S}$, then $\mathscr{W}^{\mathrm{s}}(P_1)=\mathbb{R}^2$, that is P_1 is a global sink* (see Fig. 4).

Proof. First, remark that $\mathscr{S}\subset\mathscr{B}_1$, then only P_1 exists for $(a,b)\in\mathscr{S}$, furthermore it is a local sink (Proposition 2, Fig. 3). We now show that P_1 is a global sink, that is:

$$\lim_{i\to+\infty}(\mathscr{L}_{a,b,\varepsilon})^i(X)=P_1\quad\text{for all } X\in\mathbb{R}^2.$$

Toward this aim, we show that for $(a,b)\in\mathscr{S}$, $\mathscr{L}_{a,b,\varepsilon}$ is a contraction in certain metric.

Let us remark that $\mathscr{S}$ can be equivalently written $\mathscr{S}=\{(a,b)\in\mathbb{R}^2||a|+|b|<1\}$, and also $\mathscr{L}_{a,b,\varepsilon}$ can be equivalently written: $\mathscr{L}_{a,b,\varepsilon}(x',y')=(1-aS_\varepsilon(x')+by',x')$, where $x=x'$ and $y=by'$. Thus $\mathscr{L}_{a,b,\varepsilon}(x',y')=(by'+u(x'),x')$, and $u(x')=1-aS_\varepsilon(x')$.

Let us define the metric d by: $d(M_1,M_2)=\max(|x_1-x_2|,|y_1-y_2|)$, where $M_1(x_1,y_1)$ and $M_2(x_2,y_2)$ are any points in $\mathbb{R}^2$. Since the transformation $\mathscr{L}_{a,b,\varepsilon}$ acts like Hénon's map by stretching and folding, twice the application of this transformation to a straight-line segment gives at most two folds. Thus there are at most three points N_1, N_2 and N_3 on the line segment $\overline{M_1M_2}$ such that $\mathscr{L}_{a,b,\varepsilon}(N_i)$ or $\mathscr{L}^2_{a,b,\varepsilon}(N_i)$ on the y-axis $(i=1,2,3)$. Then

$$\begin{aligned}d(\mathscr{L}^2_{a,b,\varepsilon}(M_1),\mathscr{L}^2_{a,b,\varepsilon}(M_2))\leqslant{}& d(\mathscr{L}^2_{a,b,\varepsilon}(M_1),\mathscr{L}^2_{a,b,\varepsilon}(N_1))+d(\mathscr{L}^2_{a,b,\varepsilon}(N_1),\mathscr{L}^2_{a,b,\varepsilon}(N_2))\\&+d(\mathscr{L}^2_{a,b,\varepsilon}(N_2),\mathscr{L}^2_{a,b,\varepsilon}(N_3))+d(\mathscr{L}^2_{a,b,\varepsilon}(N_3),\mathscr{L}^2_{a,b,\varepsilon}(M_2)).\end{aligned}\tag{20}$$

On the other hand, choose η, $0<\eta<1$, such that $|a|+|b|<1-\eta$, and $M_1,M_2\in\mathbb{R}^2$, such that $\overline{M_1M_2}$ and $\overline{\mathscr{L}_{a,b,\varepsilon}(M_1)\mathscr{L}_{a,b,\varepsilon}(M_2)}$ do not cross the y-axis. Then

$$\mathscr{L}_{a,b,\varepsilon}(M_i)=\mathscr{L}_{a,b,\varepsilon}(x_i,y_i)=(1+by_i-aS_\varepsilon(x_i),x_i)\quad(i=1,2,3),$$

$$\begin{aligned}d(\mathscr{L}_{a,b,\varepsilon}(M_1),\mathscr{L}_{a,b,\varepsilon}(M_2))&=\max[|b(y_1-y_2)-aS_\varepsilon(x_1)+aS_\varepsilon(x_2)|,|x_1-x_2|]\\&\leqslant\max[|b||y_1-y_2|+|a||S_\varepsilon(x_1)-S_\varepsilon(x_2)|,|x_1-x_2|].\end{aligned}\tag{21}$$

Now, it is easy to verify that $|S_\varepsilon(x_1)-S_\varepsilon(x_2)|\leqslant|x_1-x_2|$ whatever the position of $|x_1|$ and $|x_2|$, less or greater than ε. This yields

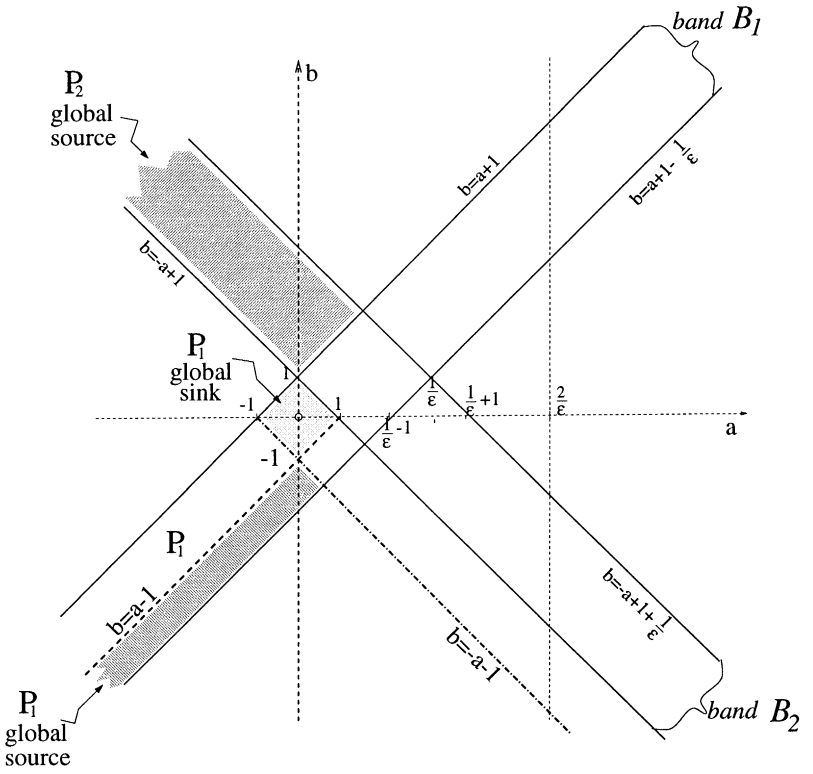

Fig. 4. Simple global behavior of $\mathscr{L}_{a,b,\varepsilon}$.

$$\begin{aligned} d(\mathscr{L}_{a,b,\varepsilon}(M_1), \mathscr{L}_{a,b,\varepsilon}(M_2)) &\leqslant \max[|b||y_1 - y_2| + |a||x_1 - x_2|, |x_1 - x_2|] \\ &\leqslant \max[(|a| + |b|)\max(|x_1 - x_2|, |y_1 - y_2|), |x_1 - x_2|] \\ &\leqslant \max[(1 - \eta)d(M_1, M_2), |x_1 - x_2|] \leqslant d(M_1, M_2). \end{aligned} \tag{22}$$

We apply this result to $(\mathscr{L}_{a,b,\varepsilon}(M_1), \mathscr{L}_{a,b,\varepsilon}(M_2))$, so we get

$$\begin{aligned} d(\mathscr{L}^2_{a,b,\varepsilon}(M_1), \mathscr{L}^2_{a,b,\varepsilon}(M_2)) &\leqslant \max[(1 - \eta)d(\mathscr{L}_{a,b,\varepsilon}(M_1), \mathscr{L}_{a,b,\varepsilon}(M_2)), |b||y_1 - y_2| + |a||S_\varepsilon(x_1) - S_\varepsilon(x_2)|] \\ &\leqslant \max[(1 - \eta)d(\mathscr{L}_{a,b,\varepsilon}(M_1), \mathscr{L}_{a,b,\varepsilon}(M_2)), (1 - \eta)d(M_1, M_2)] \\ &\leqslant (1 - \eta)d(M_1, M_2). \end{aligned} \tag{23}$$

Due to Eqs. (20) and (23) we get

$$\begin{aligned} d(\mathscr{L}^2_{a,b,\varepsilon}(M_1), \mathscr{L}^2_{a,b,\varepsilon}(M_2)) &\leqslant (1 - \eta)[d(M_1, N_1) + d(N_1, N_2) + d(N_2, N_3) + d(N_3, M_2)] \\ &= (1 - \eta)d(M_1, M_2), \end{aligned} \tag{24}$$

since M_1, N_1, N_2, N_3 and M_2 are collinear with the given order.

Consequently $\mathscr{L}^2_{a,b,\varepsilon}$ is a contraction in all the plane. We then apply the contraction-mapping theorem, which insures the existence of a unique fixed point $P \in \mathbb{R}^2$ of $\mathscr{L}^2_{a,b,\varepsilon}$ and

$$\lim_{i \to +\infty} (\mathscr{L}^2_{a,b,\varepsilon})^i(X) = P \quad \text{for all } X \in \mathbb{R}^2$$

($(\mathscr{L}^2)^i = \mathscr{L} \circ \mathscr{L} \circ \cdots \circ \mathscr{L}, 2i$-times). P is then the global sink of $\mathscr{L}_{a,b,\varepsilon}$ when (a, b) is in the region of parameters $\mathscr{S}$. As P_1 is the unique fixed point (since $\mathscr{S} \subset \mathscr{B}_1$), $P = P_1$. $\square$

Proposition 7. *If* $(a,b) \in \mathscr{B}_1$ *and* $b < a-1$, *then* $\mathscr{W}^{\mathrm{u}}(P_1) = \mathbb{R}^2$, *i.e.*, P_1 *is a global source. If* $(a,b) \in \mathscr{B}_2$ *and* $b > a+1$, *then* $\mathscr{W}^{\mathrm{u}}(P_2) = \mathbb{R}^2$, *i.e.*, P_2 *is a global source* (*see Fig.* 4).

Proof. The conditions $\{(a,b) \in \mathscr{B}_1,\ b < a-1\}$ and $\{(a,b) \in \mathscr{B}_2,\ b > a+1\}$, given in this proposition, can be equivalently written $\{(a,b) \in \mathbb{R}^2,\ |a|-|b| < -1\}$. Here, we use the same coordinate change as in the proof of the previous proposition, to get $\mathscr{L}_{a,b,\varepsilon}(x,y) = (1 - aS_\varepsilon(x) + by, x)$.

Let us set $a' = a|b'|$ and $b' = 1/b$ $(ab \neq 0)$. Then $|a|-|b| < -1$ implies $|a'/b'| - (1/|b'|) < -1$ which yields $|a'| + |b'| < 1$, that is the same condition on the parameters as in the previous proposition. Therefore, by using this previous proposition, the mapping $\mathscr{L}'_{a',b',\varepsilon'}(x,y) = (1 - a'S_{\varepsilon'}(x) + b'y, x)$ has one fixed point (in the region of parameters $|a'| + |b'| < 1$) such that its stable manifold is the entire $\mathbb{R}^2$. Now, if we use a conjugacy map $h(x,y) = (-b'y, -b'x)$ (h is a homeomorphism), one can verify that

$$\mathscr{L}_{a,b,\varepsilon} \circ h = h \circ (\mathscr{L}_{a',b',\varepsilon'})^{-1},$$

where $\varepsilon = |b|\varepsilon'$, that is, $\mathscr{L}_{a,b,\varepsilon}$ is topologically conjugate to $(\mathscr{L}'_{a',b',\varepsilon'})^{-1}$ by h. Then, $\mathscr{L}_{a,b,\varepsilon}$ and $(\mathscr{L}'_{a',b',\varepsilon'})^{-1}$ are completely equivalent in terms of their dynamics. Now, the stable manifold of $\mathscr{L}'_{a',b',\varepsilon'}$ is the unstable manifold of $(\mathscr{L}'_{a',b',\varepsilon'})^{-1}$, and Proposition 7 leads to the result.

$((\mathscr{L}'_{a',b',\varepsilon'})^{-1}$ which gives the forward iteration of a point, is defined by $(x_n, y_n) \mapsto (y_{n+1}, (x_{n+1}/b') + (a'/b')S_\varepsilon(y_{n+1}/b') - (1/b')))$. □

Remark. This concludes the first section. The interest of all these results lies in the similarity of those obtained for the Lozi-mapping. Indeed, in ('almost') all the (a,b)-plane (then in the region where the parameters a and b are classically chosen for Lozi's (or Hénon's) maps), if ε is small enough, both Lozi and $\mathscr{L}_{a,b,\varepsilon}$ mappings have the simple behavior identical. Various works on Lozi map exist, see for instance [4,9,16,17,19–21] and references therein.

The following section gives numerical evidence on the chaotic features of $\mathscr{L}_{a,b,\varepsilon}$, and comfort us on the main idea, that is, as $\varepsilon \to 0$ the global behaviors of both transformations are very close to each other.

3. Numerical investigations

Until this point, we have derived all the different fixed points of $\mathscr{L}_{a,b,\varepsilon}$ and have analyzed their stability. This was done conjointly with $\mathscr{L}_{a,b,0}$. We shall extend this study to other type of solutions through computer simulations.

We first explain how to construct the $\mathscr{L}_{a,b,\varepsilon}$ strange attractor. Then, we present various numerical results such as evidence of a fractal structure, and existence of chaotic solutions (shown with the help of bifurcation diagrams and Lyapunov exponent computation). Once the attractor is fully developed, it can disappear through a global bifurcation (while varying a parameter). This leads to the study of chaotic saddles in the last section. Through these different examples, we will again emphasize the similarities between $\mathscr{L}_{a,b,\varepsilon}$ and $\mathscr{L}_{a,b,0}$.

Our numerical investigations of the map $\mathscr{L}_{a,b,\varepsilon}$ for the usual values of parameters $a = 1.7$ and $b = 0.5$ of Lozi's map suggest the existence of strange attractor for this transformation, similar to Lozi's strange attractor. Throughout the following sections, we will denote $\mathscr{L}_{a,b,\varepsilon}$ by $\mathscr{L}_\varepsilon$.

3.1. Construction of the attractor

The transformation $\mathscr{L}_\varepsilon$ acts as Hénon's by stretching and folding in two dimensions, with coordinates x and y. The correspondence with the stretching-and-folding action can be summarized as follows:

The first step consists of a nonlinear bending in the y-coordinate (stretching of the dough in terms of kneading paradigm) given by

$$\mathscr{L}_{\varepsilon,1}(x,y) = (x, 1 - aS_\varepsilon(x) + y).$$

In the next step, a contraction in the x-coordinate is applied (folding of the dough)

$$\mathscr{L}_{\varepsilon,2}(x,y) = (bx, y),$$

the contraction factor is given by the parameter b. Finally, a reflection about the diagonal is applied (the dough is turned over)

$$\mathscr{L}_{\varepsilon,3}(x,y) = (y,x).$$

The result is

$$\mathscr{L}_{\varepsilon}(x,y) = \mathscr{L}_{\varepsilon,3}(\mathscr{L}_{\varepsilon,2}(\mathscr{L}_{\varepsilon,1}(x,y))).$$

To see the effect of repeated applications of these transformations, we take an arbitrary shape, a square for example, and apply the transformation $\mathscr{L}_{\varepsilon}$ iteratively. Fig. 5 shows this. The square is rapidly deformed, after a few iterations the attractor becomes recognizable. The following iterations do not have any visible effect on it . It is a subset of the plane, which is invariant with respect to the transformation $\mathscr{L}_{\varepsilon}$.

To have an idea on the geometry of the set of points in the plane which have orbits that are asymptotically caught by the attractor and how these sets evolve when ε changes, we give in Figs. 11(a1) and (b1) the basins of attraction of these attractors for $\varepsilon = 0$ and $\varepsilon = 0.2$.

Notice that in the $\mathscr{L}_{\varepsilon}$ case the attractor and the basin boundary are smooth.

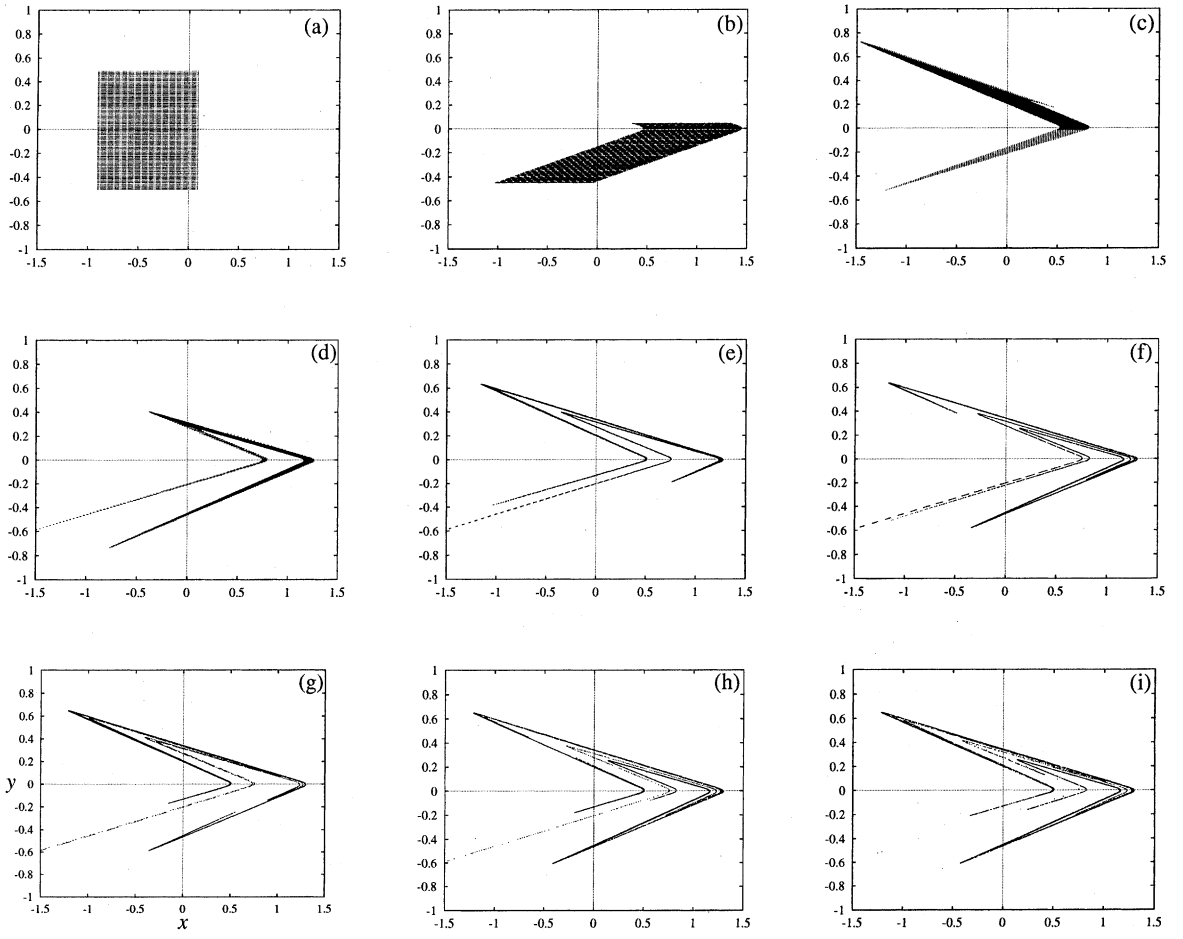

Fig. 5. Appearance of the attractor: the $\mathscr{L}_{\varepsilon}$ transformation is applied to a square (digitized by an array of 100 by 100 regularly spaced points): (a) 1; (b) 2; (c) 3; (d) 4; (e) 5; (f) 6; (g) 7; (h) 8; (i) 12 times with the parameters $\varepsilon = 0.05$, $a = 1.7$ and $b = 0.5$.

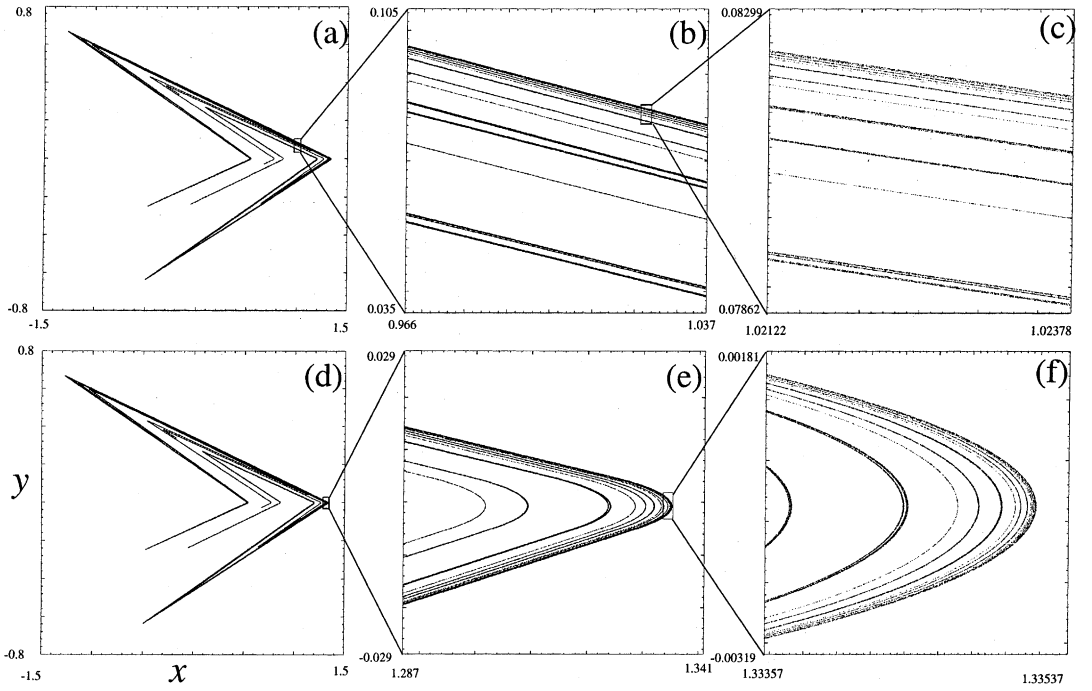

Fig. 6. Enlargement of a $\mathscr{L}_\varepsilon$ strange attractor for $\varepsilon = 0.01$, with $a = 1.7$ and $b = 0.5$. (a–c) show a zoom in the linear region, and (d–f) show a zoom in the nonlinear region. This figure, along with Figs. 7(a) and (b), and 11 have been done with the help of the software DYNAMICS [14].

3.1.1. Fractal structure

To have an idea of how the attractor for $\mathscr{L}_\varepsilon$ is strange (or fractal), we zoom in two different regions of the attractor. In Figs. 6(a–c), we zoom into a linear region, which is similar as the Lozi attractor. In Figs. 6(d–f), we zoom at the tip of the attractor, and we indeed observe a smooth folding. Notice that the structure repeats itself at all scales.

3.1.2. Bifurcation diagram for a

The route to chaos for a smooth map can be very different from the one of a piecewise linear (or nonsmooth) map. For example, for Lozi's map, no period-doubling route to chaos is allowed. The reason is the lack of continuity in the derivative of the map. Where as for the $\mathscr{L}_\varepsilon$, a period-doubling route to chaos is a typical feature. Notice that at a first glance, the global features of the bifurcation diagrams of $\mathscr{L}_0$ and $\mathscr{L}_\varepsilon$ share several common features (see Figs. 7(a) and (b)). They are almost indistinguishable. But further analysis, for example an enlargement in the region where chaos appears (see Figs. 7(c) and (d)), clearly shows a striking difference in the details of the bifurcation. In Fig. 7(c), the dynamics goes (while varying the parameter a) directly from a stable periodic orbit of period 4 to a fully developed chaotic regime. This particular type of bifurcation is called *border-collision bifurcations* [12,13]. For our map $\mathscr{L}_\varepsilon$, a typical period-doubling route to chaos is observed (see Fig. 7(d)).

3.1.3. Bifurcation sequence for ε

Now, for fixed a and b, let us vary ε. This is shown in Fig. 8. The attractor starts almost exactly like the Lozi attractor, but with almost indistinguishable smooth edges. Then the smooth aspect increases with ε. Eventually, the attractor breaks into pieces and these pieces break into more pieces.

3.1.4. Lyapunov exponent

How chaotic is the $\mathscr{L}_\varepsilon$ chaotic attractor? For a given orbit how fast nearby orbits get closer or move away? This question leads us to compute a Lyapunov exponent h. Toward this aim, we compute the derivative of $\mathscr{L}_\varepsilon$ transformation,

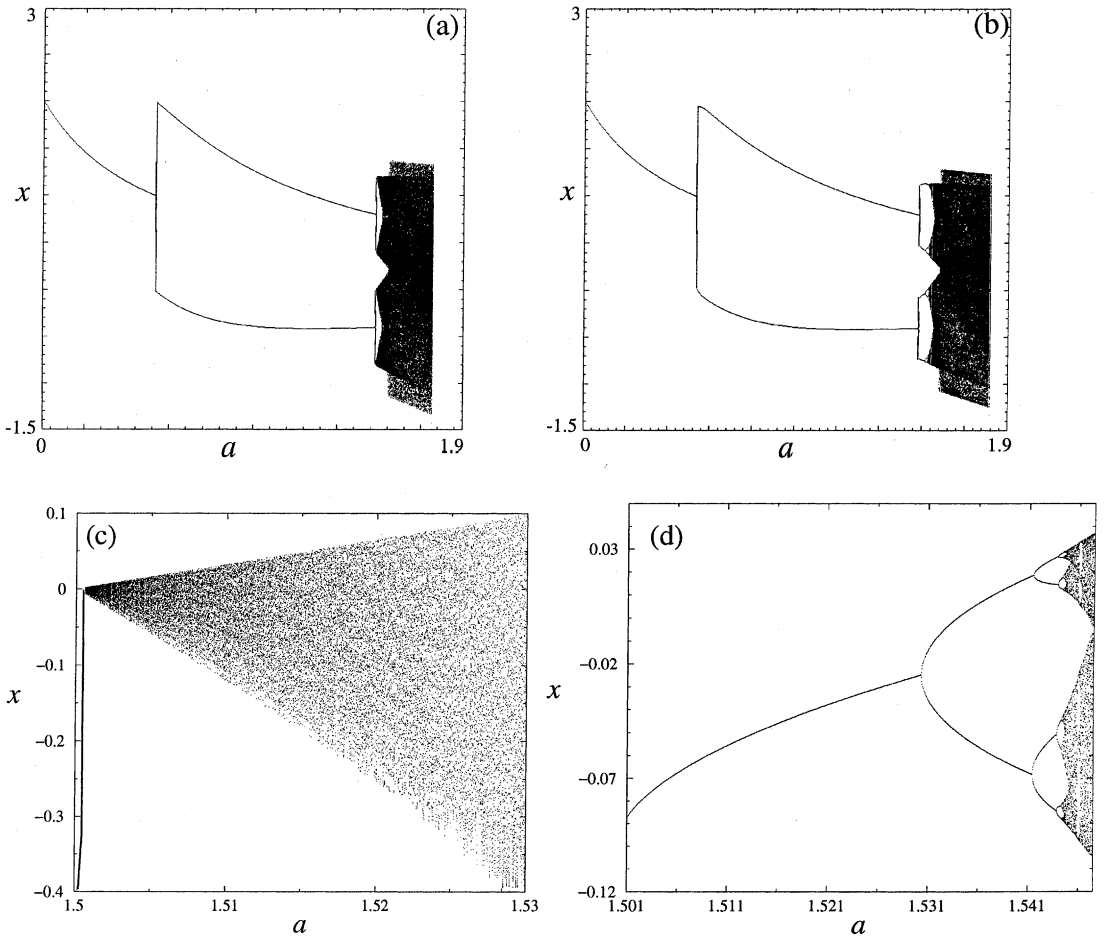

Fig. 7. Bifurcation diagrams for: (a) Lozi map; (b) $\mathscr{L}_{a,b,\varepsilon}$ with $\varepsilon = 0.1$, $a = 1.7$ and $b = 0.5$; (c) zoom in (a), there is no period-doubling route to chaos; (d) zoom in (b), there is period-doubling route to chaos.

$$D_{\mathscr{L}_\varepsilon}(x,y) = \begin{pmatrix} -a\frac{\partial S_\varepsilon(x)}{\partial x} & 1 \\ b & 0 \end{pmatrix},$$

where $\partial S_\varepsilon(x)/\partial x$ is given by Eq. (4). We can thus compute how an infinitesimally small error in a point (x,y) of the attractor is transformed by one iteration. For any arbitrary direction $(\cos(\phi), \sin(\phi))$ of the error, we compute the transformed error using the following equation:

$$\begin{pmatrix} -a\frac{\partial S_\varepsilon}{\partial x} & 1 \\ b & 0 \end{pmatrix}\begin{pmatrix} \cos(\phi) \\ \sin(\phi) \end{pmatrix} = \begin{pmatrix} -a\frac{\partial S_\varepsilon}{\partial x}\cos(\phi) + \sin(\phi) \\ b\cos(\phi) \end{pmatrix}.$$

The error amplification is then measured by the factor

$$\sqrt{\left(-a\frac{\partial S_\varepsilon}{\partial x}\cos(\phi) + \sin(\phi)\right)^2 + (b\cos(\phi))^2}.$$

By iteration and renormalizing this process we get the largest Lyapunov exponent, see Fig. 9. Several positive values of h indicate strong evidence of chaos.

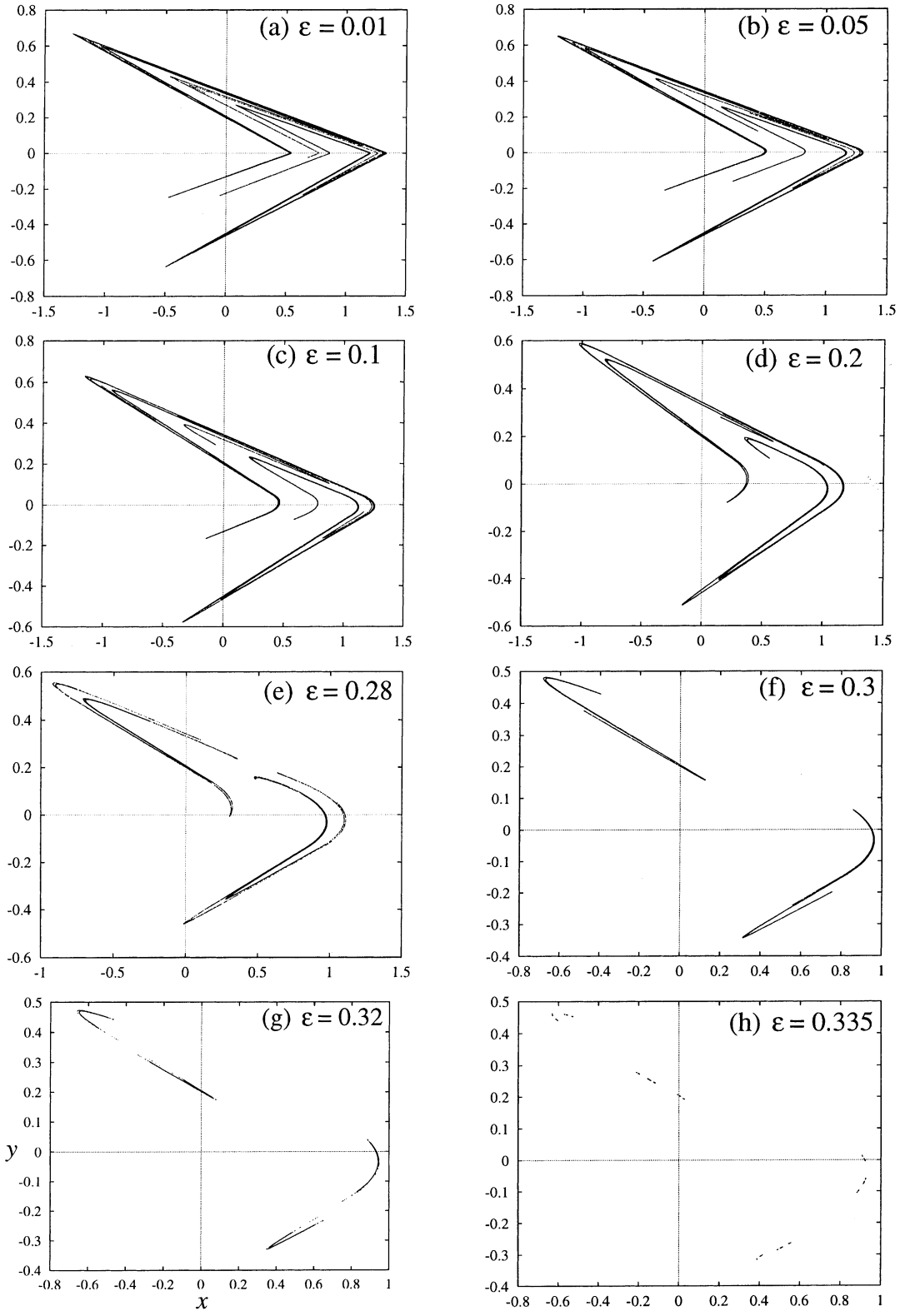

Fig. 8. The attractors for $\mathscr{L}_{a,b,\varepsilon}$ transformation, with $a = 1.7$, $b = 0.5$. ε is given in each figure.

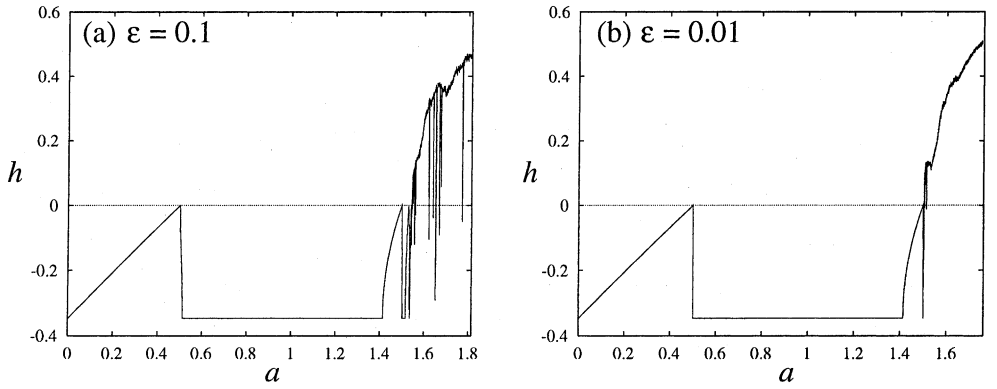

Fig. 9. Lyapunov exponent of $\mathscr{L}_\varepsilon$ mapping with $a = 1.7$, $b = 0.5$ and for: (a) $\varepsilon = 0.1$; (b) $\varepsilon = 0.01$. Values of the Lyapunov exponent h greater than 0 show evidence of chaos.

3.2. Chaotic saddle

Another interesting comparison between $\mathscr{L}_0$ and $\mathscr{L}_\varepsilon$ is to study the region in parameter space where the fully developed attractor, in both cases, suddenly disappears. This phenomenon is called boundary crisis. While varying a parameter, it occurs when a chaotic attractor collides with its own boundary basin [6,7]. Another way to understand this behavior is to follow the stable and unstable manifolds of the periodic orbit lying on the basin boundary of the attractor. After these manifolds go through tangency, the attractor has access to a new region of phase space by leaking out; it is destroyed.

We first present the boundary crisis curve when we vary both the parameters a and ε, the latter is our parameter linking $\mathscr{L}_0$ and $\mathscr{L}_\varepsilon$. This graph is presented in Fig. 10. It shows a smooth monotonic progression of ε with a. This result is not surprising [5], because the mediating orbit (the orbit going through tangency and triggering the crisis) is a fixed point and its stable manifold (also the basin boundary) does not form a Cantor set.

In Fig. 11(a1) we show the Lozi attractor together with the fixed point p (the cross) lying on the attractor's basin boundary. The stable manifold of p is also computed. It corresponds to the basin boundary of A. We have not shown the branch of the unstable manifold of p going eventually to the tangency, because the attractor A is simply on the closure of the unstable manifold of p. When we increase the parameter a to $a_c \cong 1.75$, $\mathscr{W}^u(p)$ becomes tangent to $\mathscr{W}^s(p)$. Beyond that value the chaotic attractor ceases to exist and

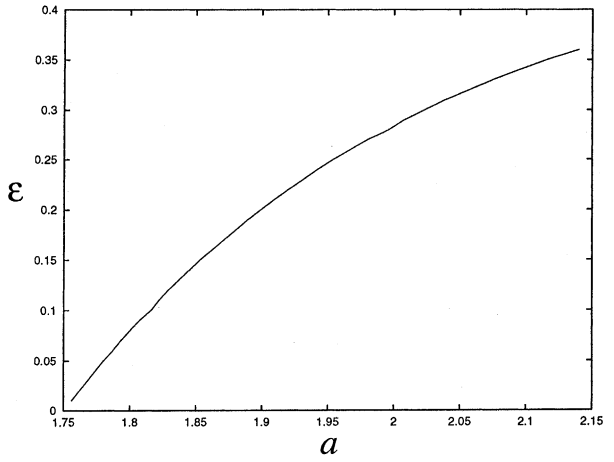

Fig. 10. Boundary crisis curve. Crossing this curve in one direction (from left to right) leads to the sudden disappearance of a chaotic attractor. Crossing the curve in the opposite direction leads to the sudden creation of a chaotic attractor.

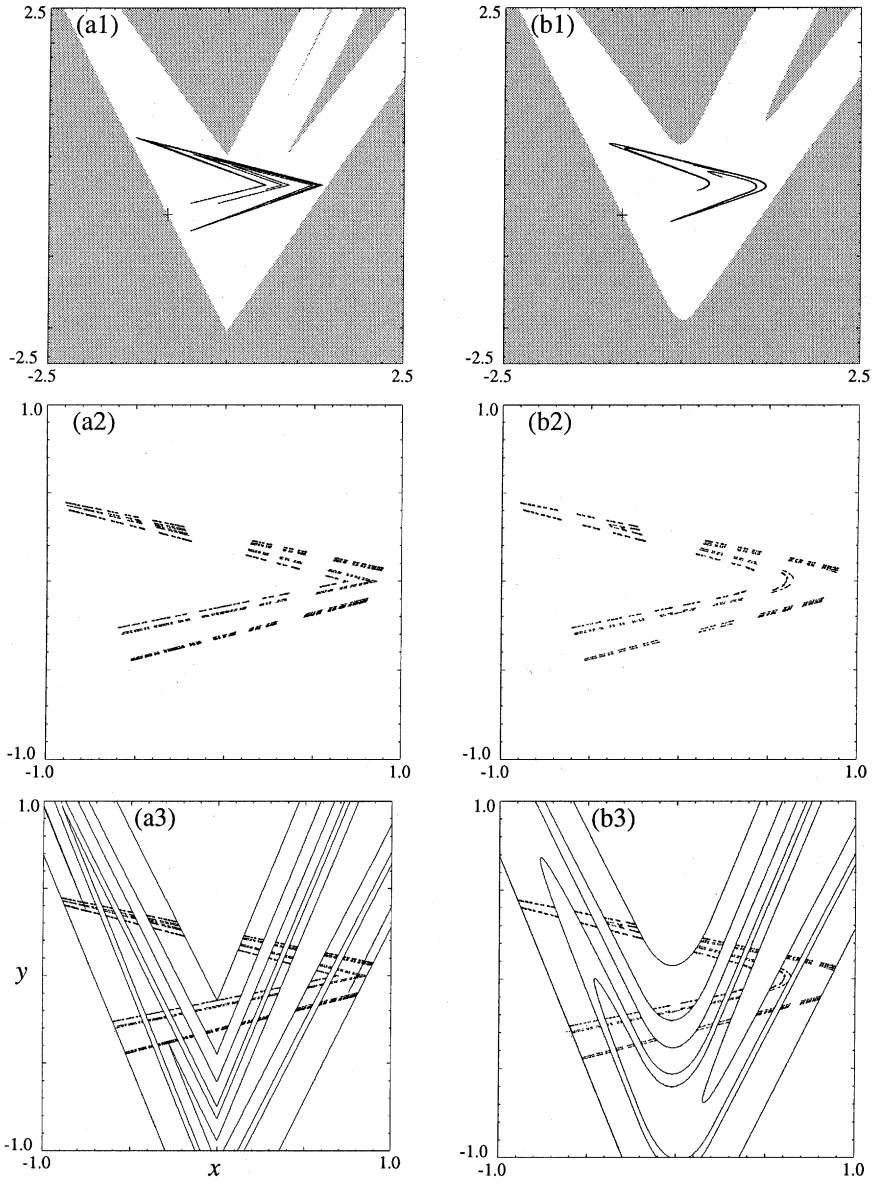

Fig. 11. Comparison of (a) $\mathscr{L}_{a,b,0}$ and (b) $\mathscr{L}_{a,b,0.2}$ before ($a = 1.7$, $b = 0.5$) and after ($a = 2.2$, $b = 0.5$) the boundary crisis. Before crisis: chaotic attractor with its basin of attraction, see (a1) and (b1). After crisis: only a chaotic saddle remains, see (a2) and (b2). Chaotic saddle with part of the stable manifold of the fixed point to show how the gaps are formed in the saddle, see (a3) and (b3). Note: only part of the stable manifold is being computed in order to help visualizing the mechanism.

almost all trajectories leak to another attractor (in this case at infinity). Fig. 11(b1) is done for the same parameter values as the previous case, except for $\varepsilon = 0.2$. Notice the smoothness of the stable manifold and of the attractor.

Just after the crisis (for $\mathscr{L}_0$ and $\mathscr{L}_{0.2}$), the chaotic attractor has suddenly disappeared, but a chaotic transient remains. This transient is due to a chaotic saddle, which is a remnant of the previously existing chaotic attractor (see Figs. 11(a2) and (b2)).

Even if this bifurcation seems to be abrupt, the union of all the recurrent sets before and after crisis is the same. The attractor just loses its attractive property and becomes a saddle. Then, while increasing a, an ensemble of gaps is created throughout the saddle in a continuous way. One way to understand that, is to look at the crossing of the stable manifold with the saddle. Since this manifold moves continuously with a,

the gaps are created continuously (see Fig. 11(a3) and (b3)). Therefore, this boundary crisis is not an explosion. An explosion is a bifurcation in which new recurrent points suddenly appear at a nonzero distance from any pre-existing recurrent points [15].

4. Conclusion

In order to prove the existence of an attractor for a given system, we often analyze oversimplified alternatives of that system which allow us to carry out proofs, but by doing so, it leads us to lose the essentials of the dynamics of the original system. We wanted to go a step further by introducing the map $\mathscr{L}_{a,b,\varepsilon}$. We derived some of its properties and compared them with the Lozi map. We obtained very good agreement with Lozi's when we take the limit $\varepsilon \to 0$. The next step would be to do a similar comparison with the Hénon map. It would be interesting to check whether, for sufficiently small ε, some weak form of quasi-hyperbolicity (similar to the results of Young [21]) could be established. Finally, an important part of this program would be to study (analytically and numerically) the notorious problems of stability islands and breakdown of hyperbolicity (see [21] and references therein). These problems form the main obstacles to an analytical treatment of continuous maps.

References

[1] Aharonov D, Devaney RL, Elias U. The dynamics of a piecewise linear map and its smooth approximation. Int J Bifur Chaos 1997;7:351–72.
[2] Aziz-Alaoui MA. On the dynamics of a C^1 approximation of the Lozi-mapping, preprint Université de Le Havre, France; 1999.
[3] Benedicks M, Carleson L. The dynamics of the Hénon maps. Ann Math 1991;133:73–169.
[4] Devaney RL. Homoclinic bifurcations and the area-conserving Hénon's mapping. J Diff Equations 1984;51:254–66.
[5] Gallas JAC, Grebogi C, Yorke JA. Vertices in parameter space: double crises which destroy chaotic attractors. Phys Rev Lett 1993;71:1359–62.
[6] Grebogi C, Ott E, Yorke JA. Chaotic Attractors in Crisis. Phys Rev Lett 1982;48:1507–10.
[7] Grebogi C, Ott E, Yorke JA. Crises sudden changes in chaotic attractors and chaotic transients. Physica D 1983;7:181–200.
[8] Hénon M. A two-dimensional mapping with a strange attractor. Comm Math Phys 1976;50:69–77.
[9] Ishii Y, Sands D. Monotonicity of the lozi family near the tent map. Comm Math Phys 1998;198:397–406.
[10] Lozi R. Un attracteur étrange(?) du type attracteur de Hénon. J Phys (Paris) 1978;39:Coll. C5 9–10.
[11] Misiurewicz M. Strange attractors for the lozi-mappings. In: Helleman RG, editor. Nonlinear dynamics, Annals of the New York Academy of Sciences 1980;357:348–58.
[12] Nusse HE, Ott E, Yorke JA. Border-collision bifurcations: an explanation for observed bifurcation phenomena. Phys Rev E 1994;49:1073–6.
[13] Nusse HE, Yorke JA. Border collision bifurcations including 'period two to period three' bifurcation for piecewise smooth systems. Physica D 1992;57:39–57.
[14] Nusse HE, Yorke JA. Dynamics: numerical explorations, 2nd ed. New York: Springer; 1998.
[15] Robert C, Alligood KT, Ott E, Yorke JA. Explosions of chaotic sets, Physica D 2000;144:44–61.
[16] Sawyer A. The dynamics of piecewise linear mapping of the plane, Ph.D. thesis, Boston, Michigan, USA; 1984.
[17] Tél T. Invariants curves attractors and phase diagram of a piecewise linear map with chaos. J Stat Phys 1983;33(1).
[18] Cao Y, Liu Z. Orientation-preserving Lozi map. Chaos, Solitons & Fractals 1998;9(11):1857–63.
[19] Cao T, Min Mao J. The non-wandering set of some Hénon maps. Chaos, Solitons & Fractals 2000;11(13):2045–53.
[20] Cao Y, Kiriki S. The basin of the strange attractors of some Hénon maps. Chaos, Solitons & Fractals 2000;111(5):729–34.
[21] Young L-S. Statistical properties of dynamical systems with some hyperbolicity. Ann Math 1998;147:585–650.